

Myosin motor Myo1c and its receptor NEMO/IKK- γ promote TNF- α -induced serine³⁰⁷ phosphorylation of IRS-1

Yoshitaka Nakamori,¹ Masahiro Emoto,¹ Naofumi Fukuda,¹ Akihiko Taguchi,¹ Shigeru Okuya,¹ Michiko Tajiri,^{2,3} Makoto Miyagishi,⁴ Kazunari Taira,⁴ Yoshinao Wada,^{2,3} and Yukio Tanizawa¹

¹Division of Molecular Analysis of Human Disorders, Department of Bio-Signal Analysis, Yamaguchi University Graduate School of Medicine, Ube 755-8505, Japan

²Core Research for Evolution Science and Technology, Japan Science and Technology Agency, Saitama 332-0012, Japan

³Department of Molecular Medicine, Osaka Medical Center and Research Institute for Maternal and Child Health, Izumi, Osaka 594-1101, Japan

⁴Department of Chemistry and Biotechnology, University of Tokyo, Bunkyo-ku, Tokyo 113-8656, Japan

Tumor necrosis factor- α (TNF- α) signaling through the I κ B kinase (IKK) complex attenuates insulin action via the phosphorylation of insulin receptor substrate 1 (IRS-1) at Ser³⁰⁷. However, the precise molecular mechanism by which the IKK complex phosphorylates IRS-1 is unknown. In this study, we report nuclear factor κ B essential modulator (NEMO)/IKK- γ subunit accumulation in membrane ruffles followed by an interaction with IRS-1. This intracellular trafficking of NEMO requires insulin, an intact actin cytoskeletal network, and the motor protein Myo1c. Increased Myo1c expression enhanced

the NEMO-IRS-1 interaction, which is essential for TNF- α -induced phosphorylation of Ser³⁰⁷-IRS-1. In contrast, dominant inhibitory Myo1c cargo domain expression diminished this interaction and inhibited IRS-1 phosphorylation. NEMO expression also enhanced TNF- α -induced Ser³⁰⁷-IRS-1 phosphorylation and inhibited glucose uptake. In contrast, a deletion mutant of NEMO lacking the IKK- β -binding domain or silencing NEMO blocked the TNF- α signal. Thus, motor protein Myo1c and its receptor protein NEMO act cooperatively to form the IKK-IRS-1 complex and function in TNF- α -induced insulin resistance.

Introduction

Insulin resistance, a condition in which the cells become resistant to the effects of insulin, is a major risk factor for type 2 diabetes as well as hypertension, dyslipidemia, and atherosclerosis (Reaven, 1988). Despite several investigations, the molecular mechanism underlying insulin resistance has not been adequately clarified. TNF- α is an adipocytokine and induces insulin resistance (Hotamisligil et al., 1993). A TNF- α signal results in the phosphorylation of Ser³⁰⁷ of insulin receptor (IR) substrate 1 (IRS-1), in turn attenuating the metabolic insulin signal (Kanety et al., 1995). Many serine kinases such as JNK, glycogen synthase kinase 3, and mammalian target of rapamycin have been reported to phosphorylate serine residues of IRS-1 (Gao et al., 2002). However, the serine kinase that precisely regulates metabolic insulin action is unclear.

After the first report of type 2 diabetes being successfully treated with high-dose salicylate in 1901 (Williamson and Lond, 1901), numerous attempts have been made to identify the target

molecules of salicylate. In 1998, salicylate was reported to be a strong inhibitor of the kinase activity of I κ B kinase (IKK) β (Yin et al., 1998). Since then, studies have focused on the IKK complex as a critical molecule for the development of insulin resistance (Yuan et al., 2001). The IKK complex consists of two catalytic subunits, IKK- α and IKK- β , and one scaffold subunit designated nuclear factor κ B essential modulator (NEMO)/IKK- γ (DiDonato et al., 1997; Nakano et al., 1998; Yamaoka et al., 1998). Among these subunits, IKK- β is a key insulin resistance molecule, as demonstrated by a study using the IKK- β knockout mouse (Kim et al., 2001). A recent study showed the IKK complex to phosphorylate IRS-1 at Ser³⁰⁷, which is associated with TNF- α stimulation and diminished insulin signaling (Gao et al., 2002). However, whether IKK- β itself physically binds to IRS-1 is uncertain. Furthermore, the role of NEMO is also unclear.

Myo1c is a motor protein that is classified as an unconventional myosin I. This class of myosins is widely distributed, having been identified in organisms from yeast to human. In adipocytes, Myo1c reportedly facilitates the recycling of vesicles containing glucose transporter 4 (Bose et al., 2002). However, little is known about the molecular mechanisms regulating motor Myo1c-cargo interactions.

Correspondence to Masahiro Emoto: emotom@yamaguchi-u.ac.jp

Abbreviations used in this paper: eGFP, enhanced GFP; IKK, I κ B kinase; IR, insulin receptor; IRS-1, IR substrate 1; NEMO, nuclear factor κ B essential modulator; shRNA, short hairpin RNA; WT, wild type.

The online version of this article contains supplemental material.

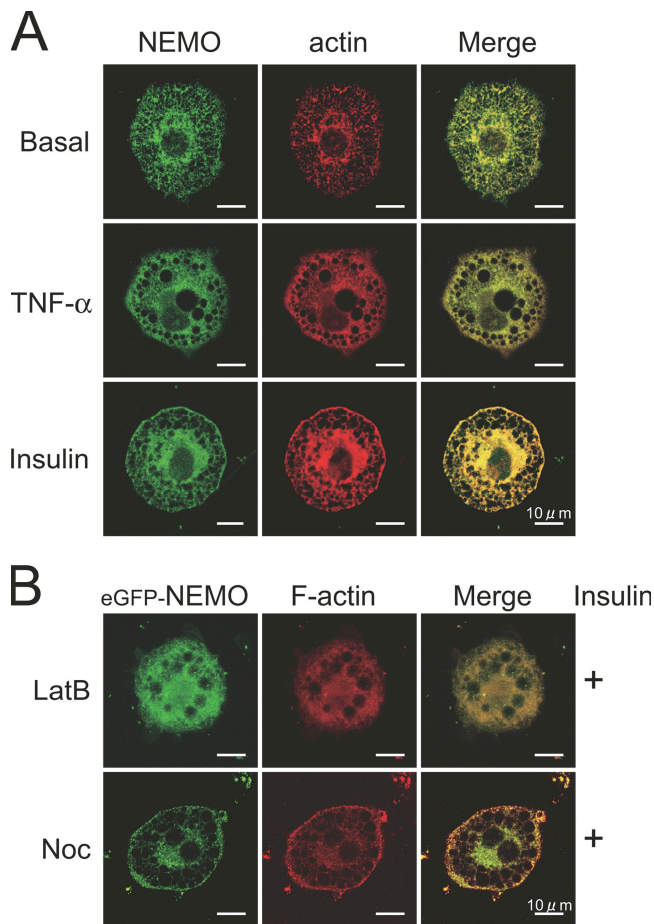


Figure 1. Intracellular localization of NEMO in 3T3-L1 adipocytes. Differentiated 3T3-L1 adipocytes (A) or adipocytes expressing eGFP-NEMO (B) were serum starved and either left untreated (A) or were pretreated with 5 μ M latrunculin B (LatB) or 30 μ M nocodazole (Noc) for 60 min (B). They were then incubated with 20 ng/ml TNF- α or 100 nM insulin for 15 min at 37°C. The cells were fixed, and F-actin was visualized by AlexaFluor596-phalloidin.

We investigated the formation of the functional complex of signaling molecules containing IKKs and IRS-1 in response to insulin. We found that NEMO functions as a motor receptor, whereas Myo1c and the actin cytoskeleton facilitate translocation of the IKK complex to membrane ruffles or to the vicinity of IRS-1. This interaction between IKKs and IRS-1 is essential for TNF- α -induced phosphorylation of IRS-1 at Ser³⁰⁷, which results in the inhibition of glucose uptake. Our present results suggest a novel mechanism whereby Myo1c–NEMO-mediated signaling complex formation plays a role in TNF- α -induced insulin resistance.

Results and discussion

NEMO translocates to membrane ruffles in response to insulin

Researchers have reported that IKK- β is crucial for TNF- α -induced IRS-1 serine phosphorylation (Gao et al., 2002; de Alvaro et al., 2004). However, the role of the NEMO/IKK- γ subunit is poorly understood. We first examined the intracellular localization of NEMO in differentiated 3T3-L1 adipocytes using

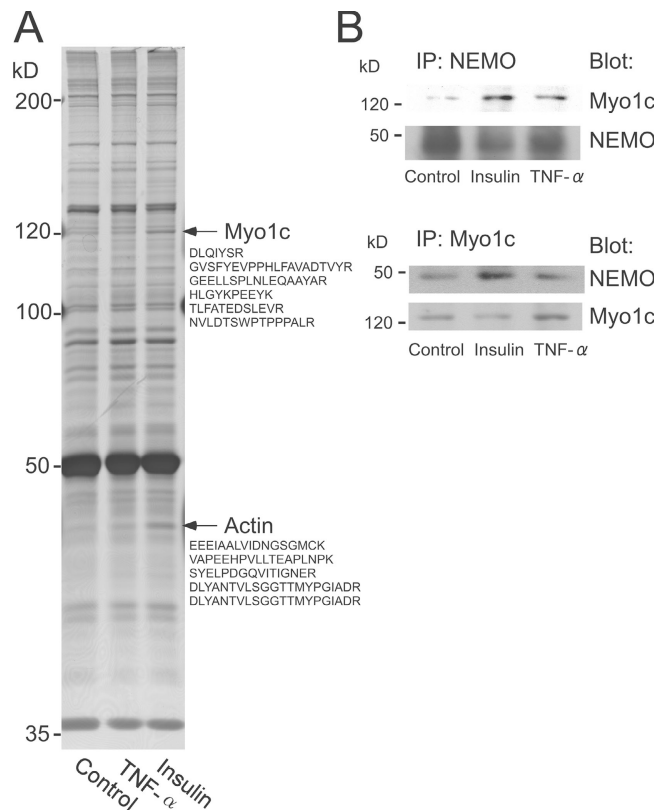


Figure 2. Insulin promotes the interaction between NEMO and Myo1c. (A) 3T3-L1 adipocytes expressing myc-tagged WT NEMO were serum starved and stimulated with 100 nM insulin or 20 ng/ml TNF- α for 20 min at 37°C. NEMO-binding proteins were immunoprecipitated with anti-myc antibody, separated by SDS-PAGE, and visualized by silver staining. Bands were proteolytically digested and analyzed by mass spectrometry. Myo1c and actin (arrows) were identified. (B) 3T3-L1 adipocytes were serum starved for 2 h and treated with 100 nM insulin or 20 ng/ml TNF- α for 20 min at 37°C. The NEMO–Myo1c interaction was determined by immunoprecipitation using anti-NEMO or anti-Myo1c antibodies.

anti-NEMO antibody. As shown in Fig. 1 A, NEMO results in a fine punctate or granular appearance throughout the cytoplasm under basal and TNF- α -treated conditions. In contrast, the addition of insulin to culture adipocytes yields the rapid translocation of NEMO to the cell periphery, especially in membrane ruffles visualized by staining with AlexaFluor596-phalloidin. This translocation is similar to that seen in other cell types (Weil et al., 2003). Interestingly, treatment with the actin depolymerizer latrunculin B inhibited NEMO translocation, whereas the microtubule disrupter nocodazole did not (Fig. 1 B). These data suggest that insulin stimulates the accumulation of NEMO at membrane ruffles through the cortical actin network.

Identification of motor protein Myo1c as a NEMO-binding partner

Because NEMO has neither an actin-binding motif nor a membrane-targeting domain, we attempted to identify NEMO-binding proteins using mass spectrometry. 3T3-L1 adipocytes were infected with an adenovirus vector containing myc-tagged full-length NEMO and were treated with 20 ng/ml TNF- α or 100 nM insulin for 20 min. The cell lysates were immunoprecipitated with anti-myc antibody. The precipitates were

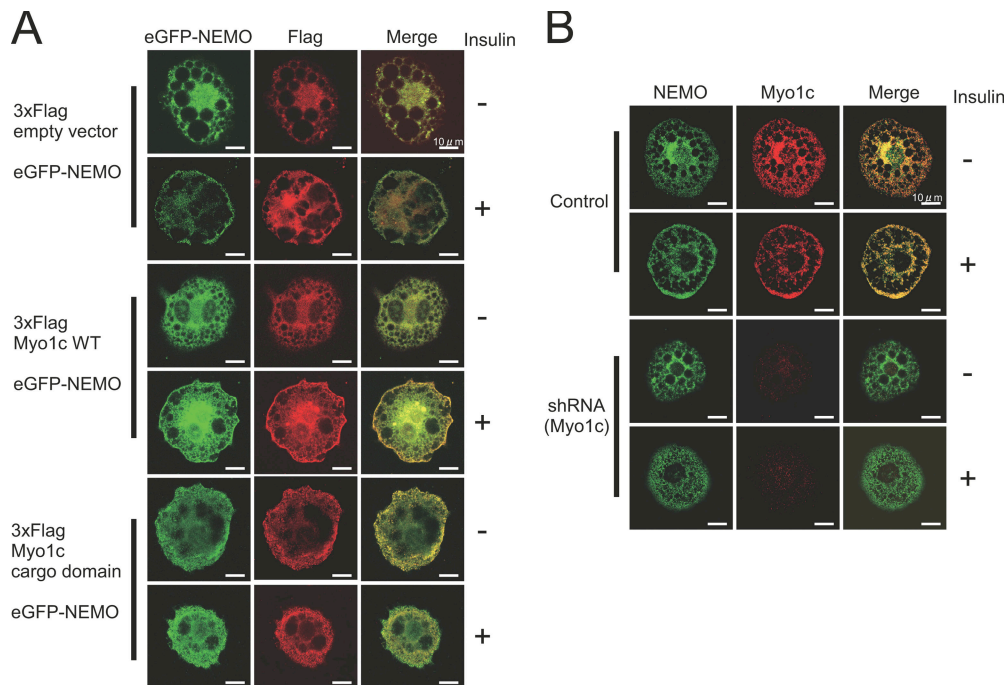


Figure 3. Effect of Myo1c expression on the intracellular localization of NEMO. 3T3-L1 adipocytes were coexpressed with eGFP-NEMO and WT Myo1c or the Myo1c cargo domain (A) or were infected with adenovirus encoding shRNA (Myo1c) or vector alone. After 2 h of serum starvation, the cells were stimulated with or without 100 nM insulin for 20 min at 37°C, stained with anti-Flag antibody followed by Cy3-labeled secondary antibody (A) or anti-NEMO antibody and anti-Myo1c antibody followed by FITC and Cy3-labeled secondary antibodies (B), and were observed by confocal microscopy.

resolved by SDS-PAGE and visualized with silver staining. With in-gel digestion followed by peptide mass fingerprinting, we identified two candidate proteins, Myo1c and actin, showing increased binding to NEMO in the presence of insulin (Fig. 2 A, arrowheads). A series of experiments were performed to confirm the interaction between NEMO and Myo1c. We first examined endogenous protein–protein interactions by immunoprecipitation using polyclonal anti-NEMO- and polyclonal anti-Myo1c-specific antibodies. As shown in Fig. 2 B, insulin treatment increased NEMO–Myo1c binding. We next confirmed this interaction using recombinant proteins in vitro. GST-tagged NEMO and His-tagged Myo1c were purified, mixed, and pulled down with each other. As shown in Fig. S1 (available at <http://www.jcb.org/cgi/content/full/jcb.200601065/DC1>), the interaction was easily detected by immunoblotting. These results suggest that NEMO and Myo1c interact directly in an insulin-dependent manner.

Myo1c conveys NEMO

Based on the results presented in Figs. 1 and 2, we hypothesized that the IKK complex containing NEMO is transported from the cytosol to membrane ruffles by Myo1c. To examine this possibility, we conducted experiments using the dominant inhibitory cargo domain of Myo1c. Overexpression of this cargo domain (residues 767–1,028) has been shown to result in the dominant inhibition of cargo binding (Bose et al., 2002). 3xFlag-tagged full-length Myo1c (wild type [WT]) or the dominant inhibitory cargo domain of Myo1c was cotransfected into culture adipocytes with enhanced GFP (eGFP)-tagged NEMO. In cells coexpressing Myo1c WT and eGFP-NEMO, NEMO showed marked

translocation to membrane ruffles with insulin stimulation. Interestingly, Myo1c WT also accumulated in the membrane and enhanced Myo1c expression, resulting in the extensive formation of membrane ruffles (Fig. 3 A). In contrast, cells expressing Myo1c cargo domain and NEMO showed the marked inhibition of insulin-stimulated NEMO translocation. Similar inhibition of NEMO translocation was observed in Myo1c knockdown cells using adenovirus encoding short hairpin RNA (shRNA [Myo1c]; Fig. 3 B).

We observed the association between NEMO and Myo1c biochemically (Fig. 2). We also found that membrane targeting of NEMO requires a motor protein, Myo1c (Fig. 3). Collectively, the data indicate the scaffold protein NEMO to be transported to membrane ruffles by the motor protein Myo1c. These observations are consistent with our aforementioned hypothesis.

Myo1c promotes IRS-1-IKK interaction and mediates Ser³⁰⁷ phosphorylation on IRS-1

A recent study showed that IKKs interact with IRS-1 and interfere with insulin signaling (Gao et al., 2002). To confirm this interaction in culture adipocytes, we first examined the localization of endogenous NEMO and IRS-1 (Fig. 4 A) or Xpress-tagged NEMO and eGFP-tagged IRS-1 (Fig. 4, B and C). In the basal state, IRS-1 was present in the cytoplasm, whereas with insulin stimulation, IRS-1 and NEMO colocalized to discrete foci in the cytoplasm as well as membrane ruffles. These observations on the intracellular localization of IRS-1 were very similar to those described in a study by Luo et al. (2005). They reported a mechanism of IRS-1 signal down-regulation involving the formation of a sequestration complex containing IRS-1 in

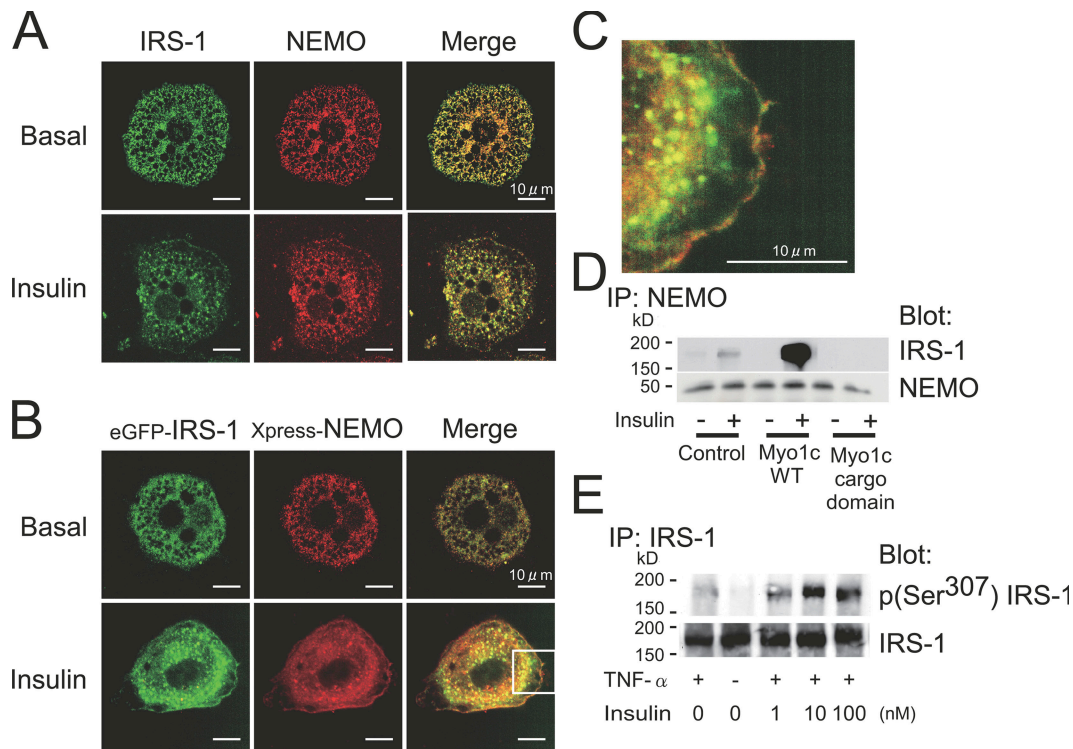


Figure 4. Myo1c modulates IRS-1-NEMO interaction. (A) 3T3-L1 adipocytes were serum starved for 2 h and stimulated with or without 100 nM insulin for 15 min at 37°C. Cells were fixed and stained with anti-IRS-1 and anti-NEMO antibody followed by FITC and Cy3-labeled secondary antibodies. (B) eGFP-tagged IRS-1 and Xpress-fused NEMO were coexpressed in 3T3-L1 adipocytes. After 2 h of serum starvation, the cells were stimulated with or without 100 nM insulin for 15 min and were then fixed. Expressed NEMO was visualized by anti-Xpress antibody and a Cy3-labeled second antibody. (C) High resolution view of the boxed area outlined in B. (D) 3T3-L1 adipocytes were infected with adenovirus encoding WT Myo1c and dominant inhibitory Myo1c. The cells were stimulated with or without 100 nM insulin for 15 min. The cell lysates were immunoprecipitated with anti-NEMO antibody, and precipitates were immunoblotted with anti-IRS-1 antibody. (E) 3T3-L1 adipocytes were left untreated or treated with 20 ng/ml TNF- α for 10 min and were incubated with various concentrations (1–100 nM) of insulin for 10 min at 37°C. The cells were lysed and immunoprecipitated by anti-IRS-1 antibody, and the precipitates were blotted with antiphospho-Ser³⁰⁷ IRS-1 and anti-IRS-1 antibody.

CHO-K1 cells. Interestingly, the large intracellular IRS-1 complexes (foci) appeared to be the negative regulatory machinery.

We next examined the direct interaction between endogenous IRS-1 and NEMO by immunoprecipitation (Fig. 4 D). Interestingly, the overexpression of Myo1c markedly increased this interaction. In contrast, cells overexpressing the dominant inhibitory cargo domain of Myo1c showed a diminished interaction. One interpretation of these findings is that Myo1c mediates the interaction by delivering NEMO to IRS-1. This explanation is supported by another set of experiments shown in Fig. S2 (A and B; available at <http://www.jcb.org/cgi/content/full/jcb.200601065/DC1>). These experiments focused on Myo1c–IKK- β and IRS-1–IKK- β associations. When NEMO was knocked down, the Myo1c–IKK- β interaction was disturbed. Similarly, the overexpression of Δ N-NEMO (detailed in the next section) diminished the IRS-1–IKK- β interaction. These results, combined with the data shown in Fig. 3, are consistent with our hypothesis that Myo1c transports the IKK complex via binding to NEMO.

Another interesting observation illustrated in Fig. 4 D was that insulin enhanced the association between IRS-1 and IKK- β . These data raise the possibility that insulin may assemble clusters of signaling molecules to facilitate the interaction between IKKs and IRS-1. To assess this possible new role of insulin,

we performed two additional experiments. First, we observed IRS-1 Ser³⁰⁷ phosphorylation induced by TNF- α after treatment with various concentrations of insulin (Fig. 4 E). Although TNF- α -induced serine phosphorylation of IRS-1 was detected within 20 min even in the absence of insulin, a low concentration of insulin markedly enhanced TNF- α -induced Ser³⁰⁷ phosphorylation. These data are consistent with the results presented in Fig. 4 D. Next, we also observed Ser³⁰⁷ phosphorylation of IRS-1 in adipocytes expressing WT Myo1c and dominant inhibitory Myo1c. Overexpression of dominant inhibitory Myo1c diminished Ser³⁰⁷ phosphorylation of IRS-1 (Fig. S3 A, available at <http://www.jcb.org/cgi/content/full/jcb.200601065/DC1>). These results show that Myo1c promotes the interaction between IRS-1 and NEMO and mediates Ser³⁰⁷ phosphorylation of IRS-1. Furthermore, a low dose of insulin and an intact actin cytoskeleton may be necessary for clustering molecules related to TNF- α to down-regulate IRS-1.

Effects of NEMO and Myo1c expression on insulin signaling and glucose transport

Because IRS-1 protein is a key mediator of insulin signaling, we next focused on the roles of Myo1c and NEMO in insulin signaling and glucose transport. We prepared WT NEMO and NH₂-terminal-deleted (Δ N; residues 101–412) NEMO constructs

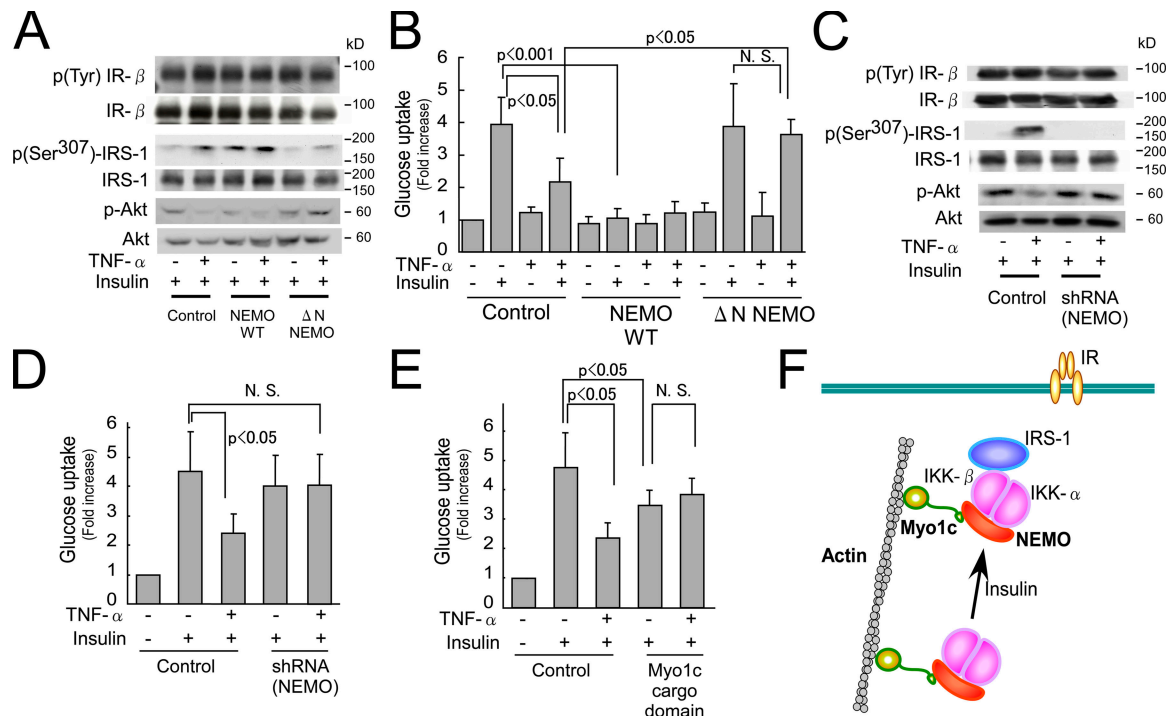


Figure 5. NEMO and Myo1c for insulin signaling and glucose uptake in 3T3-L1 adipocytes. (A–E) 3T3-L1 adipocytes were infected with recombinant adenovirus encoding wild type (WT) NEMO, Δ N-NEMO, shRNA (NEMO), Myo1c WT, Myo1c cargo domain, and vector alone (for control) at an MOI of 50. (A and C) The cells were serum starved for 2 h, treated with or without 20 ng/ml TNF- α for 15 min, and stimulated with or without 100 nM insulin for 10 min at 37°C. The cell lysates were immunoprecipitated with anti-insulin receptor β (IR- β) or anti-IRS-1 antibody, and the precipitates were immunoblotted with antiphosphotyrosine, anti-IR- β , anti-IRS-1, antiphospho-Ser³⁰⁷ IRS-1, antiphospho-Ser⁴⁷³ Akt, and anti-Akt antibodies. (B, D, and E) The cells were serum starved for 2 h in Krebs-Ringer phosphate buffer and treated with 20 ng/ml TNF- α for 4 h. Glucose uptake was measured. Each bar represents the mean \pm SD (error bars) value of at least three independent experiments. (F) Schematic model of Myo1c-mediated IRS-1- IKK complex formation.

and performed a series of experiments. The NH₂ terminal of NEMO is the IKK- β -binding site, and deletion of this site was shown to impair the binding of NEMO with IKK- β (Yamamoto et al., 2001).

First, we assessed the effects of NEMO expression on upstream insulin signal cascades in 3T3-L1 adipocytes. Overexpression of WT NEMO induced the phosphorylation of IRS-1 Ser³⁰⁷ while decreasing Akt phosphorylation in the absence of TNF- α . Overexpression of Δ N-NEMO prevented the phosphorylation of IRS-1 Ser³⁰⁷ and inhibited Akt phosphorylation. We detected no changes in the tyrosine phosphorylation of the IR β chain (Fig. 5 A). Second, we measured 2-deoxyglucose uptake in 3T3-L1 adipocytes expressing NEMO constructs. Overexpression of WT NEMO abolished insulin-stimulated glucose uptake in the absence of TNF- α . In contrast, the overexpression of Δ N-NEMO completely blocked the inhibitory effects of TNF- α (Fig. 5 B). Third, we introduced shRNA into culture adipocytes to induce specific degradation of NEMO mRNA. NEMO protein expression was decreased to 20–30% of the control level (unpublished data). As expected, the deletion of NEMO almost completely blocked the inhibition of insulin-stimulated glucose uptake by TNF- α (Fig. 5 D). Under these conditions, IR- β tyrosine, IRS-1 Ser³⁰⁷, and Akt Ser⁴⁷³ phosphorylations were examined in 3T3-L1 adipocytes. NEMO silencing by shRNA also prevented TNF- α -mediated IRS-1 Ser³⁰⁷ phosphorylation and inhibition of Akt phosphorylation without affecting IR tyrosine phosphorylation (Fig. 5 C). These data,

combined with the data presented in Figs. 3 and 4, suggest that motor protein Myo1c and its receptor protein NEMO mediate TNF- α -induced down-regulation of IRS-1 and glucose uptake.

However, it was previously shown that the overexpression of Δ N-NEMO results in the loss of IKK kinase activity (Yamamoto et al., 2001). We confirmed the inhibition of IKK kinase activity in 3T3-L1 adipocytes expressing Δ N-NEMO as well as NEMO knockdown cells (Fig. S3, B and C). These observations indicated that NEMO plays a role in assembling the IKK complex and that this step is critical for IKK kinase activity. To avoid this bias and clarify the roles of Myo1c and NEMO in glucose uptake, we conducted another experiment using Myo1c cargo domain constructs. As shown in Fig. 5 E, overexpression of the cargo domain inhibited the TNF- α -induced suppression of glucose uptake. Together, these results provide evidence that NEMO may function as a receptor molecule for Myo1c and that Myo1c promotes the TNF- α -induced suppression of metabolic insulin action. In agreement with a previous study (Bose et al., 2002), we confirmed that Myo1c cargo domain expression itself decreased insulin-stimulated glucose uptake by 30%. This may be a result of the inhibitory role of Myo1c on GLUT4 recycling (Bose et al., 2002).

Based on the aforementioned data, we propose a simple model whereby Myo1c and its receptor NEMO cooperatively facilitate IKK-IRS-1 complex formation, as illustrated in Fig. 5 F. NEMO is a scaffold protein of the IKK complex. Recent studies suggest that some scaffold proteins serve as links between

molecular motors and intracellular vesicles, thereby functioning as cargo proteins (Dorner et al., 1999; Setou et al., 2000). In contrast, our data suggest that the scaffold protein NEMO links motor and signaling molecules as cargos. It is noteworthy that Myo1c organizes the signaling complex and serves as a platform for the two distinct signals to interact (i.e., the insulin signal and the TNF- α signal mediating insulin resistance).

Finally, our results allow us to draw three conclusions. First, the motor protein Myo1c appears to participate directly in the mechanism of IRS-1–IKK complex formation in culture adipocytes. It is possible that NEMO is a molecular receptor linking motor (Myo1c) and cargo (IKK- α and - β). Second, NEMO and Myo1c may be involved in the TNF- α -induced Ser³⁰⁷ phosphorylation of IRS-1, resulting in the attenuation of insulin signaling and glucose transport. Third, Myo1c and the actin cytoskeleton may facilitate formation of the signaling molecule complex that participates in the TNF- α -induced down-regulation of IRS-1. In summary, our data suggest that Myo1c and NEMO are responsible for the mechanism of TNF- α -induced insulin resistance.

Materials and methods

Constructs

Mouse full-length NEMO and IRS-1 were cloned by RT-PCR amplification with total mRNA from 3T3-L1 adipocytes. WT and an NH₂-terminal deletion mutant of NEMO containing amino acid residues 101–412 were subcloned into pEGFP-C2, pcDNA3.1His, pET-16b, and/or pGEX-6p-1 vectors. Mouse Myo1c cDNA was purchased from DNAFORM and subcloned into p3xFLAG-CMV7.1, pET-16b, and pGEX-6p-1 vectors. IKK- α and IKK- β cDNA were gifts from H. Nakano (Juntendo University School of Medicine, Tokyo, Japan).

Reagents and antibodies

The following antibodies were used: anti-NEMO, antiphospho-Ser³⁰⁷ IRS-1, and antiphospho-Akt antibodies (Cell Signaling); anti-NEMO and anti-IRS-1 antibodies (Upstate Biotechnology); anti-Flag antibody (Sigma-Aldrich); anti-Xpress antibody (Invitrogen); and Cy3-conjugated anti-mouse IgG (Jackson ImmunoResearch Laboratories). Rabbit polyclonal anti-Myo1c antibody was generated against the peptide sequence DKSELSDKKRPE. All other antibodies were purchased from Santa Cruz Biotechnology, Inc. AlexaFluor596-phalloidin was obtained from Invitrogen. Mouse TNF- α was purchased from PeproTech.

Cell culture

3T3-L1 fibroblasts were grown in DME with 10% FBS at 37°C. The cells (3–4-d after confluence) differentiated into adipocytes with incubation in the same DME containing 0.5 mM isobutylmethylxanthine, 0.25 μ M dexamethasone, and 4 μ g/ml insulin for 3 d and were then grown in DME with 10% FBS for an additional 3–6 d.

Immunofluorescence microscopy and digital image analysis

Differentiated 3T3-L1 adipocytes were transfected by electroporation. The cells were then replated onto coverslips and allowed to recover for 48 h followed by stimulation with 100 nM insulin or 20 ng/ml TNF- α for 15 min at 37°C. Then, 5 μ M latrunculin B or 30 μ M nocodazole were added 60 min before treatment with insulin. Minimum concentrations of these agents required for disrupting the cytoskeleton in culture adipocytes were determined previously (Emoto et al., 2001). Cells were fixed with 3.7% formaldehyde in PBS, permeabilized with buffer A (0.5% Triton X-100 and 1% FBS in PBS) for 15 min, and incubated for 2 h with primary antibodies at room temperature. The cells were washed and incubated with an appropriate secondary antibody or AlexaFluor596-phalloidin for 30 min. The coverslips were washed thoroughly and mounted on glass slides. Immunostained cells were observed at room temperature with a laser-scanning confocal microscope (LSM5 PASCAL; Carl Zeiss MicroImaging, Inc.) and its two-channel scanning module equipped with an inverted microscope (Axiovert 200M; Carl Zeiss MicroImaging, Inc.). The inverted microscope

used the 63 \times NA 1.4 oil objective lens run by LSM5 processing software (Carl Zeiss MicroImaging, Inc.) and Adobe Photoshop CS2.

Preparation of adenovirus

Adenovirus producing mouse WT NEMO, deletion mutant NEMO (residues 101–412), mouse WT Myo1c, and dominant inhibitory Myo1c (residues 767–1,028) were prepared using an AdEasy Adenoviral Vector System (Stratagene).

shRNA-induced degradation of NEMO

shRNA was designed to have a 5'-AAGGATTCGAGCAGTTAGTGAGC-3' sequence. Synthetic complementary single-stranded oligonucleotide DNA was annealed, and the double-stranded DNA of the target sequence was created. This annealed DNA was inserted into a pcPUR+U6i cassette (Miyagishi and Taira, 2002), and the insert was transferred to an AdEasy Adenoviral Vector System. This shRNA system decreased NEMO protein expression to 20–30% of the control level.

Identification of NEMO-binding proteins

Myc-NEMO was expressed in 3T3-L1 adipocytes. 2 d thereafter, cells were serum starved for 2 h and stimulated with 100 nM insulin or 20 ng/ml TNF- α for 20 min. Cell lysates were prepared and immunoprecipitated with anti-myc antibody. Samples were resolved by SDS-PAGE, and proteins were visualized by silver staining. The bands were excised and subjected to in-gel digestion according to the method described by Shevchenko et al. (1996) with minor modifications. Mass spectra were acquired using a time of flight mass spectrometer (Voyager DE Pro; Applied Biosystems). The search engine for the peptide mass fingerprint was the web-based Mascot (Matrix Science).

Details of in-gel digestion. In brief, the gel pieces were washed twice in 300 μ l CH₃CN for 30 min and dried. The gel pieces were then rehydrated in 100 μ l of reduction buffer (10 mM DTT and 100 mM NH₄HCO₃) and were left standing at 56°C for 1 h. After supernatant removal, the gel pieces were incubated in 100 μ l of 50 mM iodoacetamide in 100 mM NH₄HCO₃ for 45 min at room temperature. The gel pieces were then washed in 100 μ l of 100 mM NH₄HCO₃ and dehydrated in 300 μ l of acetonitrile. After washing and dehydration (twice each), the dried gel pieces were rehydrated on ice in 100 μ l of digestion buffer (50 mM NH₄HCO₃ and 12.5 ng/ μ l each of lysylendopeptidase [Wako] and sequencing grade trypsin [Promega]) for 45 min. The supernatant was replaced with 50 mM NH₄HCO₃, and the gel pieces were incubated at 37°C overnight. The supernatant was collected, and the peptides were extracted repeatedly with a 50- μ l solution of 5% (vol/vol) formic acid and 50% (vol/vol) acetonitrile by vortexing. The combined supernatants were evaporated to dryness in a vacuum centrifuge. Resulting peptides were redissolved in 0.1% trifluoroacetic acid and absorbed onto ZipTip C18 (Millipore). Bound peptides were eluted with 50% acetonitrile and 0.1% trifluoroacetic acid. Equal amounts of the resulting peptide solution and a matrix-assisted laser desorption/ionization sample matrix solution (10 mg/ml α -cyano-4-hydroxycinnamic acid dissolved in 50% acetonitrile and 0.1% trifluoroacetic acid) were mixed on the sample target.

Pull-down assay

GST-fused NEMO and Myo1c were expressed using a pGEX-6p-1 vector in BL21 cells. His-tagged NEMO and Myo1c were expressed using a pET-16b vector in BL21 (DE3) cells. GST-fused protein and His-tagged protein were mixed in PBS and pulled down with glutathione–Sepharose beads (GE Healthcare). Protein interactions were detected by Western blotting using anti-His antibody and anti-GST antibody.

shRNA-induced degradation of Myo1c

Target sequences used in shRNA were the same as those described previously (Bose et al., 2002). Synthetic complementary single-stranded oligonucleotide DNAs were annealed to make double-stranded DNAs of the target sequences. These annealed DNA were inserted into a pcPUR+U6i cassette vector, and the plasmids were electroporated into differentiated 3T3-L1 adipocytes.

Immunoprecipitation and immunoblotting

Cells were lysed in lysis buffer (20 mM Hepes, pH 7.2, 100 mM NaCl, 1 mM EDTA, 25 mM NaF, 1 mM sodium vanadate, 1 mM benzamide, 5 μ g/ml leupeptin, 5 μ g/ml aprotinin, 1 mM PMSF, and 1 mM DTT), and the protein concentration was measured with bicinchoninic acid protein assay reagent (Pierce Chemical Co.). For immunoprecipitation, the cell lysate was preincubated with protein G–Sepharose beads at 4°C for 30 min

to remove nonspecific bound protein. Then, samples were incubated with primary antibody at 4°C for 2 h followed by incubation with protein G-Sepharose beads. Lysates and immunoprecipitates were resolved by SDS-PAGE and transferred to a polyvinylidene difluoride membrane (GE Healthcare). The membrane was preblotted in milk buffer for 1 h and immunoblotted with primary antibody for 2 h. HRP-conjugated secondary antibodies (Jackson ImmunoResearch Laboratories) were used, and proteins were visualized using an enhanced chemiluminescence substrate kit (GE Healthcare).

2-deoxyglucose uptake

Differentiated adipocytes were prepared in 24-well plates. Cells were infected with the recombinant adenoviruses. 2 d thereafter, the cells were serum starved for 2 h at 37°C in Krebs-Ringer phosphate buffer (130 mM NaCl, 5 mM KCl, 1.3 mM CaCl₂, 1.3 mM MgSO₄, and 10 mM Na₂HPO₄, pH 7.4) and were treated with or without 20 ng/ml TNF- α for 4 h. Next, the cells were stimulated with or without 100 nM insulin for 5 min, and 2-deoxyglucose uptake was determined by 2-deoxy-D-[2,6-³H] glucose incorporation. Nonspecific deoxyglucose uptake was measured in the presence of 20 μ M cytochalasin B and subtracted from each determination to obtain specific uptake. The deoxyglucose uptake was corrected using the protein amount.

In vitro kinase assay

3T3-L1 adipocytes were infected with the recombinant adenoviruses as indicated. 2 d after the infection, cells were stimulated with or without 20 ng/ml TNF- α for 5 min, and cell lysates were prepared. After adjusting the protein concentration, immunoprecipitation using anti-IKK- β antibody was performed. Precipitates were mixed with IKK substrate peptide (KKKKERLLDDRHSGLDSMKDEE; Upstate Biotechnology) and γ -[³²P] ATP. After a 10-min incubation at 30°C, samples were transferred to P81 paper (Whatman) and washed with 0.75% phosphoric acid and acetone. Radioactivity was counted using a scintillation counter.

Statistical analysis

Multiple comparisons among groups were performed using the one-factor analysis of variance test (post-hoc test; Turkey-Kramer). Results are presented as means \pm SD. Values of $P < 0.05$ were considered statistically significant.

Online supplemental material

Fig. S1 shows the results of pull-down experiments to demonstrate the direct interaction of NEMO with Myo 1c. Fig. S2 shows the effects of NEMO knockdown on Myo1c-IKK- β interaction (A) and the effects of NEMO expression on IRS-1-IKK- β interaction (B). Fig. S3 shows the effects of Myo1c expression on the TNF- α -induced phosphorylation of IRS-1 Ser³⁰⁷ (A) and the effects of WT NEMO and Δ N-NEMO expression or NEMO knockdown on IKK- β kinase activity (B and C). Online supplemental material is available at <http://www.jcb.org/cgi/content/full/jcb.200601065/DC1>.

We thank Dr. Hiroyasu Nakano for providing the IKK- α and - β constructs. We are also grateful to Dr. Teruo Nishida (Yamaguchi University Graduate School of Medicine, Yamaguchi, Japan) for allowing us to use his confocal microscope.

This work was partly supported by Grants-in-Aid for Scientific Research (KAKENHI) from the Ministry of Education, Culture, Sports, Science and Technology of Japan (15590940 and 17590934) to M. Emoto and the Research Grant for Longevity Sciences from the Ministry of Health, Labor, and Welfare of Japan (15C-8) to Y. Tanizawa.

Submitted: 12 January 2006

Accepted: 1 May 2006

References

Bose, A., A. Guilherme, S.I. Robida, S.M. Nicoloso, Q.L. Zhou, Z.Y. Jiang, D.P. Pomerleau, and M.P. Czech. 2002. Glucose transporter recycling in response to insulin is facilitated by myosin Myo1c. *Nature*. 420:821–824.

de Alvaro, C., T. Teruel, R. Hernandez, and M. Lorenzo. 2004. Tumor necrosis factor α produces insulin resistance in skeletal muscle by activation of inhibitor κ B kinase in a p38 MAPK-dependent manner. *J. Biol. Chem.* 279:17070–17078.

DiDonato, J.A., M. Hayakawa, D.M. Rothwarf, E. Zandi, and M. Karin. 1997. A cytokine-responsive I κ B kinase that activates the transcription factor NF- κ B. *Nature*. 388:548–554.

Donner, C., A. Ullrich, H.U. Haring, and R. Lammers. 1999. The kinesin-like motor protein KIF1C occurs in intact cells as a dimer and associates with proteins of the 14-3-3 family. *J. Biol. Chem.* 274:33654–33660.

Emoto, M., S.E. Langille, and M.P. Czech. 2001. A role for kinesin in insulin-stimulated GLUT4 glucose transporter translocation in 3T3-L1 adipocytes. *J. Biol. Chem.* 276:10677–10682.

Gao, Z., D. Hwang, F. Bataille, M. Lefevre, D. York, M.J. Quon, and J. Ye. 2002. Serine phosphorylation of insulin receptor substrate 1 by inhibitor κ B kinase complex. *J. Biol. Chem.* 277:48115–48121.

Hotamisligil, G.S., N.S. Shargill, and B.M. Spiegelman. 1993. Adipose expression of tumor necrosis factor- α : direct role in obesity-linked insulin resistance. *Science*. 259:87–91.

Kanety, H., R. Feinstein, M.Z. Papa, R. Hemi, and A. Karasik. 1995. Tumor necrosis factor α -induced phosphorylation of insulin receptor substrate-1 (IRS-1). Possible mechanism for suppression of insulin-stimulated tyrosine phosphorylation of IRS-1. *J. Biol. Chem.* 270:23780–23784.

Kim, J.K., Y.J. Kim, J.J. Fillmore, Y. Chen, I. Moore, J. Lee, M. Yuan, Z.W. Li, M. Karin, P. Perret, et al. 2001. Prevention of fat-induced insulin resistance by salicylate. *J. Clin. Invest.* 108:437–446.

Luo, J., S.J. Field, J.Y. Lee, J.A. Engelman, and L.C. Cantley. 2005. The p85 regulatory subunit of phosphoinositide 3-kinase down-regulates IRS-1 signaling via the formation of a sequestration complex. *J. Cell Biol.* 170:455–464.

Miyagishi, M., and K. Taira. 2002. U6 promoter-driven siRNAs with four uridine 3' overhangs efficiently suppress targeted gene expression in mammalian cells. *Nat. Biotechnol.* 20:497–500.

Nakano, H., M. Shindo, S. Sakon, S. Nishinaka, M. Mihara, H. Yagita, and K. Okumura. 1998. Differential regulation of I κ B kinase α and β by two upstream kinases, NF- κ B-inducing kinase and mitogen-activated protein kinase/ERK kinase kinase-1. *Proc. Natl. Acad. Sci. USA*. 95:3537–3542.

Reaven, G.M. 1988. Banting lecture 1988. Role of insulin resistance in human disease. *Diabetes*. 37:1595–1607.

Setou, M., T. Nakagawa, D.H. Seog, and N. Hirokawa. 2000. Kinesin superfamily motor protein KIF17 and mLin-10 in NMDA receptor-containing vesicle transport. *Science*. 288:1796–1802.

Shevchenko, A., M. Wilm, O. Vorm, and M. Mann. 1996. Mass spectrometric sequencing of proteins from silver-stained polyacrylamide gels. *Anal. Chem.* 68:850–858.

Weil, R., K. Schwamborn, A. Alcover, C. Bessia, V. Di Bartolo, and A. Israel. 2003. Induction of the NF- κ B cascade by recruitment of the scaffold molecule NEMO to the T cell receptor. *Immunity*. 18:13–26.

Williamson, R.T., and M.D. Lond. 1901. On the treatment of glycosuria and diabetes mellitus with sodium salicylate. *Brit. Med. J.* 1:760–762.

Yamamoto, Y., D.W. Kim, Y.T. Kwak, S. Prajapati, U. Verma, and R.B. Gaynor. 2001. IKK γ /NEMO facilitates the recruitment of the I κ B proteins into the I κ B kinase complex. *J. Biol. Chem.* 276:36327–36336.

Yamaoka, S., G. Courtois, C. Bessia, S.T. Whiteside, R. Weil, F. Agou, H.E. Kirk, R.J. Kay, and A. Israel. 1998. Complementation cloning of NEMO, a component of the I κ B kinase complex essential for NF- κ B activation. *Cell*. 93:1231–1240.

Yin, M.J., Y. Yamamoto, and R.B. Gaynor. 1998. The anti-inflammatory agents aspirin and salicylate inhibit the activity of I κ B kinase- β . *Nature*. 396:77–80.

Yuan, M., N. Konstantopoulos, J. Lee, L. Hansen, Z.W. Li, M. Karin, and S.E. Shoelson. 2001. Reversal of obesity- and diet-induced insulin resistance with salicylates or targeted disruption of I κ B. *Science*. 293:1673–1677.